Nuclear Instruments and Methods in Physics Research B 533 (2022) 50–55

Contents lists available at ScienceDirect

Nuclear Inst. and Methods in Physics Research, B

journal homepage: www.elsevier.com/locate/nimb

A novel activation technique for integrated cross section measurements using accelerator mass spectrometry

Austin D. Nelson *, Adam M. Clark, Thomas L. Bailey, Lauren K. Callahan, Philippe Collon

Department of Physics, University of Notre Dame, Notre Dame, IN 46556, United States

ARTICLE INFO

Keywords:
41Ca
AMS
In-cathode activation
Early solar system

ABSTRACT

^{41}Ca ($t_{1/2} = 9.94 \times 10^4$ yrs) is an important stellar radionuclide and its production in the Early Solar System from various irradiation scenarios can help determine the viability of models of early stellar processes. A novel reaction technique has been under development and recently tested at the Nuclear Science Laboratory at the University of Notre Dame. This technique utilizes an "in-cathode" reaction method, where natural CaF_2 material is packed into an ion source sample holder (cathode) and then irradiated and subsequently measured using Accelerator Mass Spectrometry (AMS) without the need for chemical processing afterward. The setup for the irradiation was performed using a ^{3}He beam to measure the reaction ^{nat}Ca(^{3}He,x)^{41}Ca. Initial AMS results suggest additional complexity due to ion source sputtering rates and geometry, which will need to be explored further.

1. Introduction

The presence of short-lived radionuclides in the Early Solar System are key to understanding the production processes that went into its formation some 4.6 billion years ago. Analysis of meteoritic material has found an increased presence of the abundances of daughter nuclei of the short-lived radionuclides ^{10}Be, ^{26}Al, ^{36}Cl, ^{41}Ca, ^{53}Mn, and ^{60}Fe, among others [1,2]. The wide variance of half-lives of these materials, which range from hundreds of thousands of years to several million years, can allow for a fine-tuning of the processes producing these isotopes.

Several sources of production for these radionuclides have been proposed, mostly stemming from two distinct frameworks: stellar nucleosynthesis processes from a massive star exploding as a supernova from somewhere outside the Solar System, or local spallation from the early protosun in the forms of ionized H and He atoms [1,3,4]. The latter of these scenarios can be predicted with models which need input on the specific target compositions and cross sections for the relevant pathways of production [5]. Due to its relatively shorter half-life compared to the other stellar radionuclides, ^{41}Ca ($t_{1/2} = 9.94 \times 10^4$ yrs [6]) can offer strong constraints on model calculations, particularly with ^{3}He-induced reactions, which have been shown to possibly contribute a considerable fraction of the total production of ^{41}Ca in the Early Solar System [4,5,7]. However, the cross sections for these types of reactions are rare and only a handful of data points exist for the production of ^{41}Ca through the reaction of ^{nat}Ca with ^{3}He [5]. Therefore, in order to help constrain models, experimentally determined cross section measurements must be made.

Previous measurements for the production of short-lived radionuclides have been performed using activations on either thin films with gas activation chambers [8,9] or target stacks [5] and have used chemical extraction or separation followed by Accelerator Mass Spectrometry (AMS) to measure the amount of rare isotope produced to calculate a cross section. Aside from the rigorous setup for these various irradiation procedures, the main drawbacks of these techniques are the need for chemistry steps to isolate the element of choice and for the addition of a carrier solution to get a reasonable amount of material to be able to measure it through AMS methods.

Here, we present a unique "in-cathode" method for activation of material for integrated cross section measurements using AMS. While the concept for an "in-cathode" activation of material has been previously attempted [10,11], the new cathode holder design and activation method, combined with gamma spectrometry and AMS measurement, are a completely different and novel approach. By using an MC-SNICS ion source cathode packed with material as a target, this method has the advantage of ease of use for target preparation, omitting any chemical sample preparation after the activation has taken place, thereby eliminating some uncertainties that would otherwise need to be incorporated into a measurement. The cathode was used as a target for irradiations, placed in a gamma counting station to measure any quickly decaying radionuclides, and then put into an ion source for measurement of isotopic ratios.

* Corresponding author.
E-mail address: anelso12@nd.edu (A.D. Nelson).

https://doi.org/10.1016/j.nimb.2022.10.016
Received 18 April 2022; Received in revised form 28 September 2022; Accepted 13 October 2022
Available online 7 November 2022

We performed initial tests of this method using the reaction ^{nat}Ca(^{3}He, x)^{41}Ca on a cathode filled with CaF_2 powder and used AMS to measure the ratio of ^{41}Ca/^{nat}Ca in the sample. This reaction was used not only due to the accessibility of sample and standard Ca material, but also because previous experiments, using a different technique, have shown good agreement with theoretical cross section models [5]. Here, we will focus on the development of the technique and provide some initial results.

2. Calculations

In order to estimate the required irradiation time to reach a desired ^{41}Ca/^{nat}Ca ratio, we need to consider that the number of ^{41}Ca atoms produced in the reactions ^{nat}Ca(^{3}He,x)^{41}Ca is given by:

$$N_{41_{Ca}} = \frac{\rho_{CaF_2} \cdot d \cdot N_A}{M_{CaF_2}} \cdot I_{3_{He}} \cdot t \cdot \sum_n a_n \sigma_n \tag{1}$$

where ρ_{CaF_2} is the measured density of the CaF_2 powder packed in the sample, d is the depth the beam particle can travel in the material, N_A(=6.022 × 10^{23} mol^{-1}) is Avogadro's constant, M_{CaF_2}(=78.07 g/mol) is the molar mass of CaF_2, I_{3He} is the current of incoming ^{3}He particles, and t is the time of irradiation. The sum considers all stable Ca isotopes, their abundance a_n, and the cross section σ_n of the respective reaction(s) producing ^{41}Ca. However, the cross section is not constant over the entire energy range and therefore must be integrated instead. The yield of ^{41}Ca particles is therefore dependent on both the differential cross section and the material stopping power ($\frac{dE}{dx}$).

The differential cross section can be estimated using TALYS 1.8 and Fig. 1 shows the predicted cross sections for the reaction of each stable Ca isotope. The stopping power was calculated using SRIM [12] which is based on the semi-empirical Bethe-Bloch formula. With these values constantly changing, Equation (1) must be written as an integral, which then gives

$$N_{41_{Ca}} = \frac{\rho_{CaF_2} \cdot N_A \cdot I_{3He} \cdot t}{M_{CaF_2}} \cdot \sum_n a_n \int_{E_0}^{E_{beam}} \frac{\sigma_n(E)}{\frac{dE}{dx}(E)} dE \tag{2}$$

The ratio of ^{41}Ca to ^{nat}Ca can then be expressed as

$$\frac{N_{41_{Ca}}}{N_{nat_{Ca}}} = \frac{I_{3_{He}} \cdot t}{d \cdot A} \cdot \sum_n a_n \int_{E_0}^{E_{beam}} \frac{\sigma_n(E)}{\frac{dE}{dx}(E)} dE \tag{3}$$

The SRIM stopping power function was fitted with a simple power function while the TALYS prediction for each Ca isotope was fitted with a fifth order polynomial, which were chosen based on the reduced chi-squared. This method was performed for each Ca isotope considering the natural abundances. All irradiation times were calculated by aiming for an isotopic ratio of around ^{41}Ca/^{nat}Ca = 2.0 × 10^{-10} based on statistics and predetermined capabilities of the AMS system.

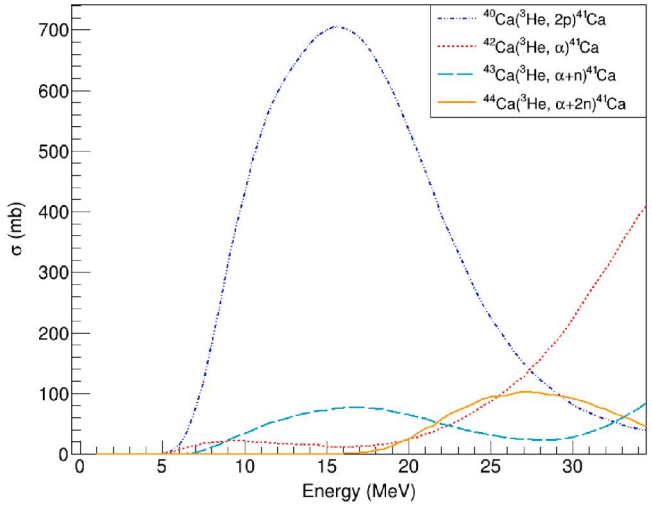

Fig. 1. TALYS1.8-predicted cross sections for the production of ^{41}Ca for the various natural Ca isotopes. ^{46}Ca and ^{48}Ca are not included as their reaction cross sections are zero within this energy range.

3. Experimental methods

Previous experimental setups encountered issues with the beam not directly hitting the cathode material [10,11] due to it being such a small target, so a unique cathode holder was designed and created to combat this issue.

3.1. Materials

In order to hold the cathodes directly in the way of the beam, three separate cathode holders were designed and machined to be attached to a target ladder as shown in Fig. 2. The main parts of the holders were made of polyester plastic for insulating purposes. A tantalum shield was placed in front of each cathode holder with a 1 mm hole drilled in the center. This hole was precision measured to be in line with the opening of the cathode in order to maximize hitting beam on the cathode material. An isolated thin, metal washer was placed after the tantalum opening and before the cathode, with a small hole drilled in the side to set a small screw onto the outside of the washer. A suppression voltage of −300 V was then able to be applied to the washer via this lead to contain any electrons that would escape from interactions of the beam with the cathode material. The copper cathode with the CaF_2 powder sat at the end of the holder, embedded within the plastic to isolate it from all other pieces. A small hole was then drilled into either side of the insulating piece to allow a screw to pin the cathode in place and pick off the charge collected from the cathode when bombarded by the beam. Both the suppression and cathode screws were attached by separate wire cables and sent to individual BNC feed-throughs.

For the irradiations, a small scattering chamber was set up and aligned to the existing beamline. The chamber had eight equidistant openings around the outside, an opaque bottom plate, and a solid aluminum lid on top. The cathode holders were attached to a target ladder, along with a small Faraday cup for beam tuning purposes. This target ladder was connected to a hand-driven linear motion device which was then attached to the scattering chamber at an opening situated 90 degrees from the beam entrance point. A picture of the setup is shown in Fig. 3. Two blank-off pieces with three BNC feed-through connections each provided current outputs for all three cathodes, current output readings of the Faraday cup and target ladder, and a suppression voltage.

In order to ensure alignment of the beam and cathode, a 2″ quartz viewer was attached at the back end of the scattering chamber. A scope on the beamline, originally used to set up the scattering chamber, was then used to view the position of the cathode for each irradiation and small adjustments could be made by hand with the linear motion device for alignment with beam center.

3.2. Cathode packing

All cathodes used for this experiment were made from vacuum-cleaned high-purity Cu and purchased from National Electrostatics Corp. (NEC). Cathodes were weighed before being packed with CaF_2 powder, purchased from Alfa Aesar (99% purity). All tools used to pack the powder were cleaned beforehand with ethanol and deionized water and baked in a vacuum oven at 120 °C for two hours to prevent any contamination. After packing, cathodes were weighed again to determine the amount of CaF_2 powder and then sealed in the back with a small piece of Cu wire. All cathodes were weighed a final time so that they could later be compared to their weights after irradiation, as a

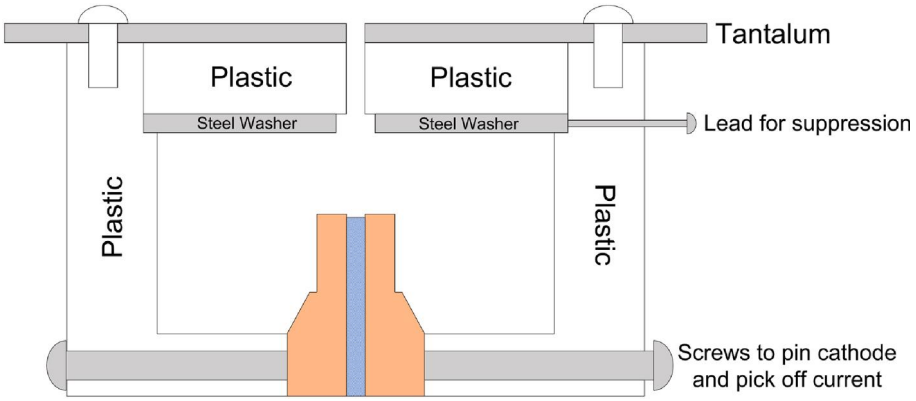

Fig. 2. Schematic for the designed cathode holder, electrically isolated by plastic material. Beam is collimated by the tantalum shield and impinged upon the cathode material. A small suppression voltage is applied to the washer for electron suppression.

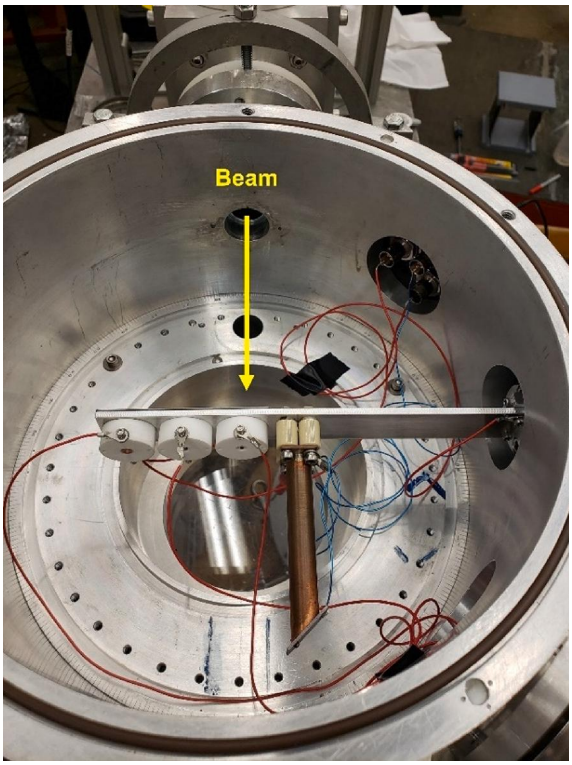

Fig. 3. Picture of the scattering chamber setup for irradiations. Three cathode holders and a small Faraday cup are attached to a target ladder which is moved in and out by a hand-driven linear motion device.

check for any losses. It should be noted that there was no discernible difference in mass from before and after the irradiations.

3.3. Irradiations

The irradiations were performed at the Nuclear Science Laboratory (NSL) at the University of Notre Dame in September 2020. A helium duoplasmatron ion source was used to produce a $^{3}He^{-}$ beam which was then accelerated using the 10 MV FN Tandem accelerator and the 2+ charge state was selected by the analyzing magnet. Each irradiation was performed under vacuum in the scattering chamber, which contained the target ladder and three individual cathode holders, as described in Section 3.1. The irradiation of each cathode was performed at a specific beam energy, as determined by the terminal voltage (+/- 20 kV) and NMR-calibrated magnetic field in the analyzing magnet. These values are given in Table 1. The highest energy beam was selected and tuned first and all other energies were found by scaling the terminal voltage of the accelerator and magnets of the system to the appropriate energy.

Table 1
Irradiation parameters for all activated samples with predicted isotopic ratios calculated using TALYS-predicted cross sections and measured AMS isotopic ratios.

Sample Number	Beam Energy [MeV]	Charge Collected [nC]	Irradiation Time [s]	Predicted $^{41}Ca/^{nat}Ca$ [x 10^{-10}]	Measured $^{41}Ca/^{nat}Ca$ [x 10^{-10}]
1*	24.54	7256.5	1800	———	———
2	25.22	1213.3	480	2.05	3.3(5)
3	25.22	1218.3	480	2.06	2.9(5)
4	23.74	1153.7	780	2.05	1.7(4)
5+	22.25	1126.5	660	2.07	———
6	20.82	1160.7	300	2.15	2.1(4)
7	19.35	1128.6	240	2.07	3.9(5)
8	17.88	1173.9	420	2.06	3.8(5)
9	16.43	1282.9	360	2.07	2.9(4)
10	14.88	1499.9	1140	2.13	2.8(4)
11	13.46	1779.9	1200	2.06	3.5(5)
12	11.97	2460.4	960	2.12	3.1(4)
13	10.50	3660.1	1860	2.00	2.2(3)
14	9.00	7766.6	4680	2.00	2.6(4)

*Sample 1 was tested with an alpha beam for 30 min as proof of concept and to test the setup.
+Sample 5 had a systematic shift in the analyzing magnet causing unreliable data.

For each energy, the beam was tuned to the Faraday cup attached to the target ladder to maximize beam current on the cup and minimize current on the target ladder, allowing for the narrowest possible beam. The target ladder was then moved and adjusted via the scope and quartz viewer so that the cathode was centered on the beamline. The cathode was then irradiated for a predetermined amount of time based on the incoming beam current and theoretical cross section models, as described in Section 2. The total beam on target was monitored continuously, the charge was integrated, and its output was digitized. The total charge collected and predicted abundances are given in Table 1.

3.4. Gamma counting station

Irradiated cathodes were placed in an off-line counting station immediately after irradiation to measure the activity of any decaying isotopes produced during the activation. This also allows for corrections in isotopic ratios from the beam impinging on the Cu cathode. The cathodes were positioned on a specially designed holder and placed inside a four-inch-thick lead castle lined with oxygen-free copper to minimize background. Activity measurements were performed with a large volume HPGe Canberra detector. The gamma spectra were

calibrated for both energy and efficiency using ^{60}Co, ^{133}Ba, ^{137}Cs, and ^{152}Eu sources with known activities.

Each cathode was placed in the lead castle for two, 15-minute runs as soon as possible after the end of beam time, and again 48 h later. Any dead-time losses were small and corrected using the live-time of the detector and activity calculations were corrected for the time elapsed from the end of the irradiation.

3.5. Accelerator mass spectrometry

As a proof of concept, the ratio of ^{41}Ca/^{nat}Ca was measured using AMS, with a similar setup and measurement procedure to previous AMS measurements [8,9]. CaF^- was extracted from an MC-SNICS ion source and accelerated using the FN Tandem accelerator set to a voltage of 8.685 MV. A combination of foil and gas stripping was used and a charge state of 9+ was chosen using the analyzing magnet, for a total beam energy of 84.1 MeV, with a charge state yield of around 6.1%. The beam was then sent through a Wien filter for isotopic filtering and through a 90-degree Browne-Buechner spectrograph magnet filled with 3.0 Torr of N_2 for isobaric separation, with a beamline transmission of around 24.6%. Ions were identified using a parallel grid avalanche counter (PGAC) filled with 3.0 Torr of isobutane for position detection and an ionization chamber (IC) filled with 12.0 Torr of isobutane for energy loss.

The ^{40}Ca current was continuously measured on offset Faraday cups on both the low and high-energy side while ^{41}Ca was injected into the accelerator and sent down the beamline to the detector system. This process involved the jumping of the bias voltage on the injection magnet, the details of which can be found in [13]. Each irradiated cathode was run for twelve consecutive, 15-minute runs for a total of three hours. A blank cathode was run for an hour before and after each sample cathode to account for background and a cathode with a known, standard isotopic ratio, obtained from Purdue's PRIME Lab (^{41}Ca/^{nat}Ca = 3.7 × 10^{-10}), was run periodically to normalize measurements and monitor any systematic changes.

4. Results & discussion

4.1. Gamma spectrometry

A representative gamma spectrum is shown in Fig. 4 with several peaks labeled. It should be noted that the ^{137}Cs peak was from a contaminated lead brick in the surrounding lead castle and was seen on all calibration and sample spectra. While most of the signals are weak, there are several isotopes that were produced from the ^{3}He beam impinging on the Cu cathode, including ^{61}Cu, ^{65,66}Ga, and ^{63}Zn. The activity of these isotopes can be calculated using

$$A(t) = \frac{N_\gamma}{\epsilon(E_\gamma)\cdot I_\gamma \cdot t_L} \tag{4}$$

where N_γ is the number of events in the peak corrected for background, $\epsilon(E_\gamma)$ is the efficiency of the detector at the specific energy of the gamma line, I_γ is the gamma ray intensity, and t_L is the live-time of the data acquisition. The original number of particles produced can then be found by

$$N_0 = \frac{A(t) \bullet \ln 2}{t_{1/2}} \bullet e^{\frac{t_l \bullet \ln 2}{t_{1/2}}} \tag{5}$$

where $t_{1/2}$ is the half-life of the isotope and t_l is the amount of time since the end of irradiation. Using the measured half-lives from NNDC [14,15] and the TALYS-predicted cross sections for each reaction, the total amount of current hitting the Cu cathode can be calculated using a similar method described in Section 2. Equation (2) can then be used to calculate the amount of current incident on the Cu cathode by using the density (ρ_{Cu} = 8.96 g/cm^3) and molar mass (M_{Cu} = 63.55 g/mol) for Cu and summing over the two stable isotopes (^{63}Cu and ^{65}Cu). Just like Section 2, the cross sections were calculated using TALYS 1.8 and the stopping power of ^{3}He in Cu was calculated using SRIM [12].

Table 2
The measured activities and calculated beam current incident on the Cu cathode for a subset of relevant gamma rays shown in Fig. 4.

Gamma Isotope	Gamma Energy [keV]	Reported Half-Life [s]	Calculated Activity [Bq]	Calculated Current [pnA]
^{61}Cu	282.9	12020.4	710(121)	0.0275(60)
^{61}Cu	656.0	12020.4	687(120)	0.0267(59)
^{61}Cu	1185.2	12020.4	574(133)	0.0223(60)
^{66}Ga	833.5	34164.0	565(72)	0.0314(58)
^{66}Ga	1039.2	34164.0	543(47)	0.0301(48)

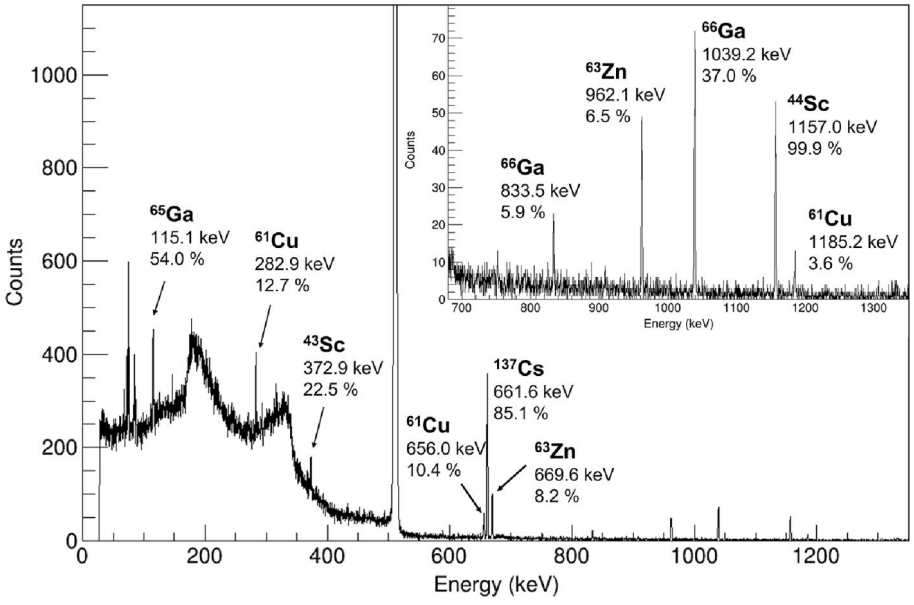

Fig. 4. Representative gamma spectrum for an irradiated cathode (Sample 3 in this case). There are several isotopes produced from the irradiation of the Cu cathode and a few Sc isotopes seen from the production of ^{3}He on ^{nat}Ca.

The results for the calculated amount of beam hitting the Cu cathode using some of the more well-known peaks in the gamma spectrum can be found in Table 2. For this particular cathode, the current on target was around 1.5 pnA, so the current hitting the Cu cathode was around 1–2% of the total beam. These results were consistent for all other irradiated cathodes.

4.2. Initial accelerator mass spectrometry

The AMS measurement of the ratio of $^{41}Ca/^{nat}Ca$ was plagued with several issues during the run which led to larger than expected uncertainties. One major issue was low counting statistics due to the extremely low currents coming from the ion source. Each cathode would only produce around 1.0–4.0 nA of beam current out of the source on the low-energy side, over an order of magnitude less than originally seen during previous ^{41}Ca development. This could have been due to a worn-out ionizer or some alignment issue with the ion source.

Another major issue throughout the run was the drifting of the pressure in the gas-filled magnet (GFM) due to a leak somewhere in the O-ring connection of the spectrograph. This caused shifts of the energy loss and position signals and required the magnet to periodically be pumped out and filled back to its original pressure of 3.0 Torr N_2. To account for the shifting GFM pressure and its effect on the spectra, the centroid of the ^{41}K region was tracked for each run and any shift from the original position was applied similarly to the ^{41}Ca region and cuts. This was done for all samples, blanks, and standards.

Finally, due to the jumping of magnet bias to inject ^{40}Ca into the offset Faraday cup [13], some ^{40}Ca made it into the detector. While this region was separated from ^{41}Ca, it contributed to an increase in background levels, bringing the blank $^{41}Ca/^{nat}Ca$ ratio up to $(9.2 \pm 0.4) \times 10^{-11}$. Representative spectra are shown in Fig. 5 to highlight this effect.

Each sample cathode was measured for twelve, 15-minute runs, the isotopic ratio for each run was calculated and then plotted vs time, as shown in Fig. 6. For the higher energy activated samples, the ratio was fairly steady above background while the lower energy activated samples produced ratios that started out high and then diminished as more material was sputtered. If we consider a more convoluted depth-profile of the material (one that is dependent on the cross section and energy loss, smeared out by any geometric sputtering effects and energy straggling), we would expect to see the isotopic ratio start off high and remain somewhat consistent as the material is first sputtered and then start to taper off as we go further into the material. Eventually, there will be a point where none of the material being sputtered was activated and the ratio should decrease to the level of a blank, as is most evident in the case of Sample 14 shown in Fig. 6. However, statistics and measurement times were not enough to observe the full effect of this behavior in most other cathodes.

While a traditional AMS isotopic ratio is calculated by averaging the ratio over several runs, we are not able to do that here since it is not constant throughout the material. Therefore, final isotopic ratios were calculated by integrating the total ^{41}Ca events for the 12 runs, divided by the total number of ^{40}Ca events (corrected for the ^{40}Ca abundance) and total measured time. The average background level, seen in the blank cathodes before and after each sample, was then subtracted and a normalization factor of 4.1 +/- 0.3, calculated from the standard, was applied. The measured ratios of $^{41}Ca/^{nat}Ca$ are shown in the last column of Table 1. It should be noted that due to an unexpected shift in the analyzing magnet, measurements of Sample 5 became inconsistent and have therefore been omitted.

Due to the differences in depth of activated material, the isotopic ratios for the higher energy activated samples tend to be inflated above the predicted values since it is fairly clear that the whole depth of the activated material was not measured within the three hours. However, there remains a large uncertainty about any geometrical sputtering effects from the ion source. If sputtering craters tend to grow conically (or possibly even more irregular), it could be possible to start sputtering

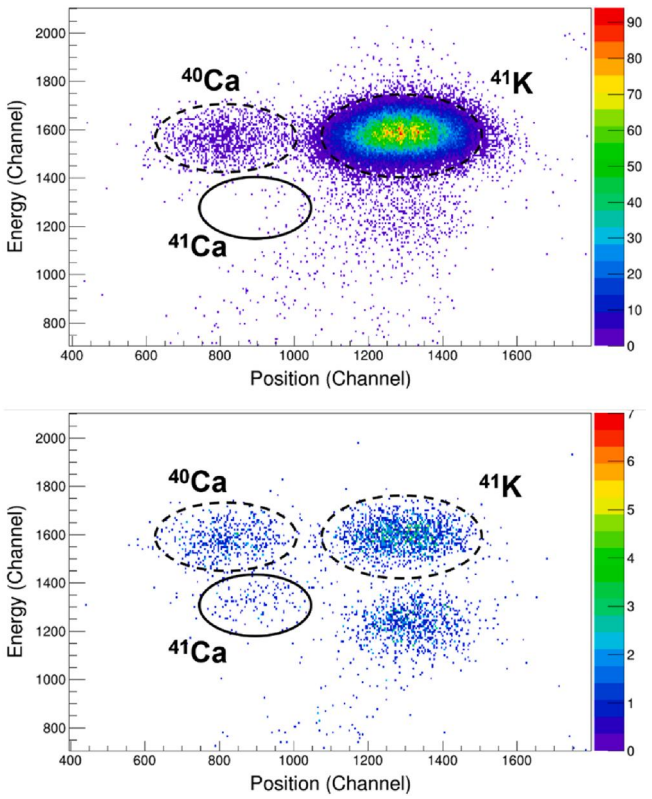

Fig. 5. Representative detector spectra of energy loss in Anode 2 vs position for a one-hour measurement on a blank (top) and standard (bottom) cathode.

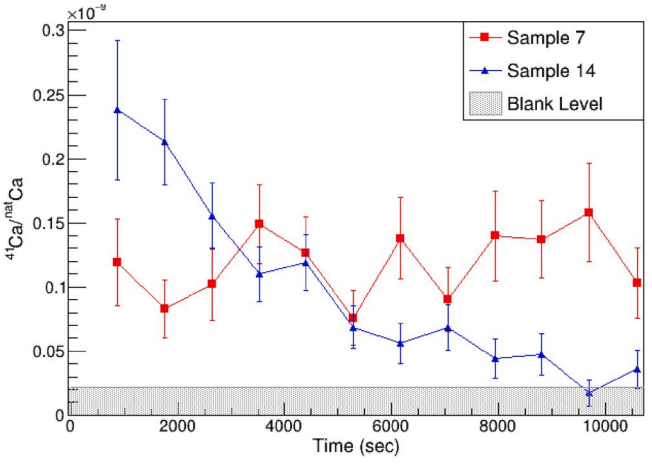

Fig. 6. Raw $^{41}Ca/^{nat}Ca$ isotopic ratios of two samples with each data point calculated from a 15-minute run. The blank level was found from the average of an hour-long run before and after each sample cathode.

inactivated material in the center of the cathode while still sputtering activated depths more around the outside; an effect that could lead to both under-and over-estimations of results. Therefore, a more unfocused Cs beam may be more beneficial for these types of measurements. While it is currently unknown how these sputtering effects will affect the overall isotopic ratios, it should be noted that within the course of the three-hour measurements, only Sample 14 (with an activated depth of around 50 μm) seemed to go down to a background level. Given that the activated depth of the samples range from only 50–300 μm, it could be that geometric effects are minimal, but future studies should be conducted to try to quantify any effects the geometry would have on the overall isotopic ratios.

5. Conclusions and future work

This "in-cathode" technique demonstrates the unique ability to combine a thick target activation with an AMS measurement without the need for any chemistry steps on the material after the activation. Gamma spectrometry can be used to correct for the ^{3}He current impinging on the Cu sample holder instead of the sample material. Future AMS measurements with this technique need to be performed in such a way that the entire activated sample is measured while also considering any geometric effects from the sputtering of the cathode material. However, for a first attempt, the process seems to work well and can be more successful after some fine-tuning and obtaining a more accurate AMS measurement. Furthermore, this technique is by no means limited to the production of ^{41}Ca and can be useful for measurements of other short-lived radionuclides.

The AMS group at Notre Dame has performed a new round of similar activations and an AMS measurement using the lessons learned from this first attempt. Further developments of ^{41}Ca capabilities have also improved the sensitivity of the system and the issue with low beam output has been resolved with a source realignment and a new ionizer. Analysis of the results from this improved run are underway with plans to present the details and results in a future journal article.

Declaration of Competing Interest

The authors declare that they have no known competing financial interests or personal relationships that could have appeared to influence the work reported in this paper.

Acknowledgements

We would like to thank George Jackson at PRIME Lab for supplying us with all the AMS standard materials used for measurements. We would also like to thank Jerry Lingle of the NSL for helping design and machine all the required pieces for the new cathode holders and the many ND graduate students who sat shift on the FN for experiments. This work is supported by the National Science Foundation under Grant No. PHY-2011890 and the Nuclear Regulatory Commission award number 31310019 M0037.

References

[1] G.R. Huss, B.S. Meyer, G. Srinivasan, J.N. Goswami, S. Sahijpal, Stellar sources of the short-lived radionuclides in the early solar system, Geochim. Cosmochim. Acta 73 (2009) 4922–4945.
[2] M. Gounelle, M. Chaussidon, T. Montmerle, Irradiation in the early solar system and the origin of short-lived radionuclides, C.R, Geoscience 339 (2007) 885–894.
[3] M. Gounelle, F.H. Shu, H. Shang, A.E. Glassgold, K.E. Rehm, T. Lee, The irradiation origin of beryllium radioisotopes and other short-lived radionuclides, Astrophys. J. 640 (2) (2006) 1163–1170.
[4] I. Leya, A.N. Halliday, R. Wieler, The predictable collateral consequences of nucleosynthesis by spallation reactions in the early solar system, Astrophys. J. 594 (1) (2003) 605–616.
[5] G. F. Herzog, M. W. Caffee, T. Faestermann, R. Hertenberger, G. Korschinek, I. Leya, R. C. Reedy, J. M. Sisterson, Cross sections from 5 to 35 MeV for the reactions ^{nat}Mg(^{3}He,x)^{26}Al, Al(^{3}He,x)^{26}Al, ^{nat}Ca(^{3}He,x)^{41}Ca, and ^{nat}Ca(^{3}He,x)^{36}Cl: Implications for early irradiation in the solar system, Meteoritics & Planetary Science 46 (2011) 14–1446.
[6] C.D. Nesaraja, E.A. McCutchan, Nucl. Data Sheets 133 (2016) 1.
[7] T. Lee, F.H. Shu, H. Shang, A.E. Glassgold, K.E. Rehm, Protostellar cosmic rays and extinct radioactivities in meteorites, Astrophys. J. 506 (2) (1998) 898–912.
[8] T. Anderson, M. Skulski, L. Callahan, A. Clark, A. Nelson, P. Collon, G. Chmiel, T. Woodruff, M. Caffee, Measurement of ^{34}S(^{3}He, p)^{36}Cl cross sections for nuclide enrichment in the early solar system, Phys. Rev. C 101 (2020), 025801.
[9] M. Bowers, Y. Kashiv, W. Bauder, M. Beard, P. Collon, W. Lu, K. Ostdiek, D. Robertson, Measurement of the ^{33}S(α, p)^{36}Cl cross section: Implications for production of ^{36}Cl in the early solar system, Phys. Rev. C 88 (2013), 065802.
[10] V. Araujo-Escalona, L. Acosta, E. Andrade, L. Barrón-Palos, O. de Lucio, F. Favela, A. Huerta, E. Lopez, P.S. Rita, C. Solis, E. Chávez, Study of the ^{28}Si(d, α)^{26}Al nuclear reaction at low energies, Phys. Procedia 90 (2017) 421–428.
[11] V. Araujo-Escalona, L. Acosta, E. Andrade, L. Barrón-Palos, C. Cantó, F. Favela, A. Huerta, M.E. Ortiz, C. Solís, E. Chávez, The ^{28}Si(d, α) reaction, J. Phys. Conf. Ser. 730 (2016).
[12] J. Ziegler, J. Biersack, The stopping range of ions in matter (SRIM) (2013).
[13] M. Skulski, T. Anderson, L. Callahan, A. Clark, A. Nelson, D. Robertson, E. Stech, P. Collon, Recent developments in the AMS system at the Nuclear Science Laboratory: Impacts on radionuclide sensitivities and current capabilities, Nucl. Instrum. Method. Phys. Res. B 488 (2021) 30–36.
[14] K. Zuber, B. Singh, Nucl. Data Sheets 125 (2015) 1.
[15] E. Browne, J. Tuli, Nucl. Data Sheets 111 (2010) 1093.